DTU Library

400-GHz wireless transmission of 60-Gb/s nyquist-QPSK signals using UTC-PD and heterodyne mixer

Yu, Xianbin; Asif, Rameez; Piels, Molly; Zibar, Darko; Galili, Michael; Morioka, Toshio; Jepsen, Peter Uhd; Oxenløwe, Leif Katsuo

Published in:
IEEE Transactions on Terahertz Science and Technology

Link to article, DOI:
10.1109/TTHZ.2016.2599077

Publication date:
2016

Document Version
Peer reviewed version

This article has been accepted for inclusion in a future issue of this journal. Content is final as presented, with the exception of pagination.

400-GHz Wireless Transmission of 60-Gb/s Nyquist-QPSK Signals Using UTC-PD and Heterodyne Mixer

Xianbin Yu, *Senior Member, IEEE*, Rameez Asif, Molly Piels, Darko Zibar, Michael Galili, Toshio Morioka, Peter U. Jepsen, and Leif K. Oxenløwe

***Abstract*—We experimentally demonstrate an optical network compatible high-speed optoelectronics THz wireless transmission system operating at 400-GHz band. In the experiment, optical Nyquist quadrature phase-shift keying signals in a 12.5-GHz ultradense wavelength-division multiplexing grid is converted to the THz wireless radiation by photomixing in an antenna integrated unitravelling photodiode. The photomixing is transparent to optical modulation formats. We also demonstrate in the experiment the scalability of our system by applying single to four channels, as well as mixed three channels. Wireless transmission of a capacity of 60 Gb/s for four channels (15 Gb/s per channel) at 400-GHz band is successfully achieved, which pushes the data rates enabled by optoelectronics approach beyond the envelope in the frequency range above 300 GHz. Besides those, this study also validates the potential of bridging next generation 100 Gigabit Ethernet wired data stream for very high data rate indoor applications.**

***Index Terms*—Photomixing, THz photonics, THz wireless communication, ultradense wavelength-division multiplexing (UD-WDM), unitravelling carrier photodiode (UTC-PD).**

I. Introduction

OPTICAL fiber communication technologies have enabled spectrally efficient high data rates in the wired networks, and 100- and 400-GbE links will be soon deployed in the backbone by telecommunication service providers [1]. In comparison, wireless data rates grow even faster and are quickly approaching 100 Gb/s [2], particularly driven by an increasing demand for high bit-rate wireless services, such as wireless access of rich content media, wireless transmission of ultrahigh definition video (UHD), wireless download of large volume data, etc. Fig. 1 illustrates some potential application scenarios of high-speed photonic-wireless communication technologies, typically in the population-intensive, and, hence, data-intensive areas. For instance, future E-health systems transporting large volume of reliable medical data would be one of the scenarios. Beside those, newly emerging ultrafast wireless applications, e.g., superfast wireless downloading and supercomputing, superfast board-to-board interconnecting, and superfast wireless smart home [see Fig. 1(b)] are also driving wireless techniques towards extremely high speed beyond 100 Gb/s. As an example, transmission of uncompressed UHD requires up to 80-Gb/s data rate. Supporting such fast wireless data rates would definitely require very large radio frequency (RF) bandwidth, the radiation spectrum naturally falls into the THz (0.3–10 THz) range. Therefore, there has been an increasing interest in exploring THz frequencies for accommodating bandwidth-hungry high-speed wireless communications.

We summarize up-to-date research efforts on the progress of high-speed THz wireless communication systems [3]–[28], as shown in Fig. 2. In the footprint map, RF carrier frequencies have been increased from W-band (75–110 GHz) till 600 GHz,

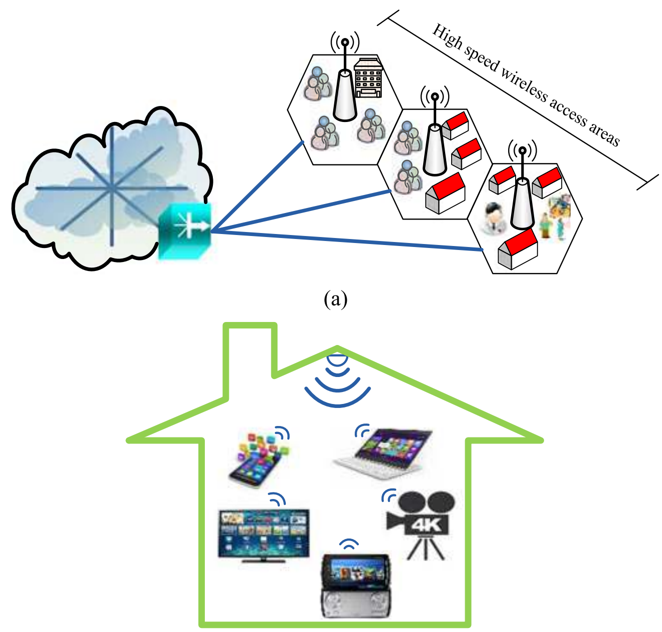

(a)

(b)

Fig. 1. Some potential application scenarios of high-speed wireless communication technologies. (a) Ultradense deployment areas, e.g., population- and data-intensive areas and E-health applications. (b) Superfast wireless in smart home.

Manuscript received February 19, 2016; revised May 17, 2016 and July 9, 2016; accepted August 5, 2016. This work was supported by the ERC-PoC Project TWIST within the European Union's Horizon 2020 Research and Innovation Program (641420-TWIST-ERC-2014-PoC).

X. Yu is with the College of Information Science and Electronic Engineering, Zhejiang University, Hangzhou 310027, China, and also with the DTU Fotonik, Department of Photonics Engineering, Technical University of Denmark, Kgs. Lyngby DK-2800, Denmark (e-mail: xyu@zju.edu.cn).

R. Asif is with the Department of Engineering, University of Cambridge, Cambridge CB2 1TN, U.K. (e-mail: ramasif@fotonik.dtu.dk).

M. Piels, D. Zibar, M. Galili, T. Morioka, P. U. Jepsen, and L. K. Oxenløwe are with the DTU Fotonik, Department of Photonics Engineering, Technical University of Denmark, Kgs. Lyngby DK-2800, Denmark (e-mail: mopi@fotonik.dtu.dk; dazi@fotonik.dtu.dk; mgal@fotonik.dtu.dk; tomo@fotonik.dtu.dk; puje@fotonik.dtu.dk; lkox@fotonik.dtu.dk).

Color versions of one or more of the figures in this paper are available online at http://ieeexplore.ieee.org.

Digital Object Identifier 10.1109/TTHZ.2016.2599077

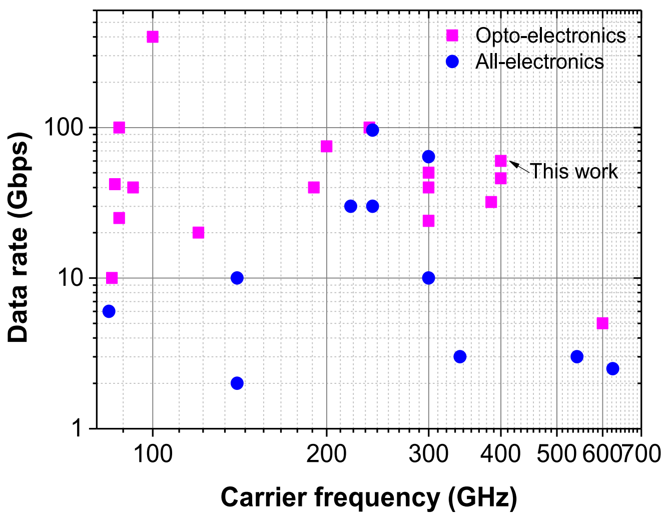

Fig. 2. Data rate versus carrier frequency in the range of 100–700 GHz.

in order to explore more available bandwidth in higher frequency bands for carrying high-speed information. There are two main approaches adopted to develop these THz wireless communication systems: all-electronics approach employing electronic devices for both THz emitter and receiver [10]–[16] and optoelectronics approach based on photonic generation of high-speed THz signals. We can see that the optoelectronics approach has made significant contributions on delivering very high data rates, particularly above 10 Gb/s. So far the highest single-transmitter bit rate of 100 Gb/s has been achieved at the W-band [8] and 237 GHz [13], and maximum 64 Gb/s based on all-electronics approach [25] and 50 Gb/s based on optoelectronics approach [26] in the frequency range of 300–400 GHz and above have been reported.

In this paper, we experimentally demonstrate an optoelectronics THz wireless communication system operating at 400-GHz band, and carrying scalable data rates derived from optical signals in a 12.5-GHz ultradense wavelength-division multiplexing (UD-WDM) grid. THz carriers are generated by heterodyne photomixing of free-running optical sources. This photonic generation of millimeter wave and THz signals is transparent to modulation formats used in existing WDM optical networks. To demonstrate this compatibility of our system with optical networks, spectrally efficient optical Nyquist channels with quadrature phase shift keying (QPSK) data planned for commercial 100 GbE [29] is used. We also investigate the scalability of our system by applying single, three, and four channels. At the receiver side, real-time capable second heterodyne down conversion [28] is used to demodulate the signals. 400-GHz wireless transmission of up to aggregated 60-Gb/s data is successfully achieved for four-channel 7.5-Gbaud QPSK signals, which is enabled by using commercially available state-of-the-art THz transceivers. 60-Gb/s THz wireless transmission is so far the highest photonics-enabled data rate in the frequency range above 300 GHz. This study, therefore, pushes data rates enabled by optoelectronics approach beyond the envelope of state of the art, paving the way of deploying THz wireless communication for very high data rate wireless access.

II. Experimental Setup

The experimental system is shown in Fig. 3. We create a multichannel QPSK optical signal by employing a 100-kHz continuous-wave (CW) laser array with frequency stability ± 1.5 GHz and power stability +/-0.03 dB over 24 h. In order to decorrelate neighboring channels, 25-GHz-spaced even-order and odd-order wavelengths are separately modulated by in-phase (I) and quadrature (Q) baseband signals from an arbitrary waveform generator (AWG), and a fiber-based delay line is used. The half-wave voltage of 32-GHz IQ modulators is 3 V. Nyquist pulse shaping is electrically performed by applying a square root raised cosine filter with 0.1 roll-off factor in the AWG, and the data sequence has a pseudorandom binary sequence length of 2^7-1. Interleaving the channels formulates a multichannel data stream in a 12.5-GHz UD-WDM grid. Subsequently, all the optical channels with baseband modulation are boosted by an Erbium-doped fiber amplifier (EDFA), filtered by a 1-nm optical filter for suppressing out-of-band noise, and then coupled with an optical local oscillator (LO) with 100-kHz linewidth for heterodyne generation of THz signals. In this experiment, a single channel is generated by simply switching on one CW laser, but keeping the others off. In our experiment, a commercially available broadband bow-tie antenna integrated unitravelling photodiode (UTC-PD) from Nippon Telegraph and Telephone Electronics (NTT-Electronics) is used as THz photomixing emitter, due to its extremely fast photoresponse [30]. Before launching into the UTC-PD, the optical signals are polarized to minimize the polarization dependence of the UTC-PD. In the wireless domain, we use a pair of THz lens with 25-dBi gain, effective focal length of 54 mm, and diameter of 37 mm to collimate the THz beam for free-space transmission. The first lens collects the THz emission from the UTC-PD and collimates it into a parallel beam, and the second lens focuses the parallel THz beam onto a THz diagonal horn antenna.

In the receiver, a THz mixer operating in the frequency range of 325–500 GHz (Virginia Diodes) is used to down convert the received THz signal into intermediate frequency (IF) range. The mixer is driven by a 12-time frequency multiplied 31–36 GHz electrical LO signal and has 22-dB conversion loss. The IF output is amplified by a chain of electrical amplifier with 6-dB noise figure and 68-dB gain, and then sampled, analyzed, and demodulated with a real-time sampling scope (63-GHz Keysight DSOZ634A Infiniium).

III. Results and Discussions

In the experiment, the THz wireless propagation distance is fixed at 50 cm, and the path loss is less than 2 dB when the THz beam is collimated by the THz lenses. When the incident total optical power to the UTC-PD (equal power for the baseband and the optical LO) is 13 dBm, THz emission power is estimated as -21 dBm by using a Pyroelectric THz power meter. After the electrical heterodyne at the receiver mixer, the IF channels are individually down converted into the 20-GHz band. This IF signal is measured using the real-time scope and real-time processed by digital signal processing (DSP) algorithms in the vector signal analyzer software employed [31]. The embedded

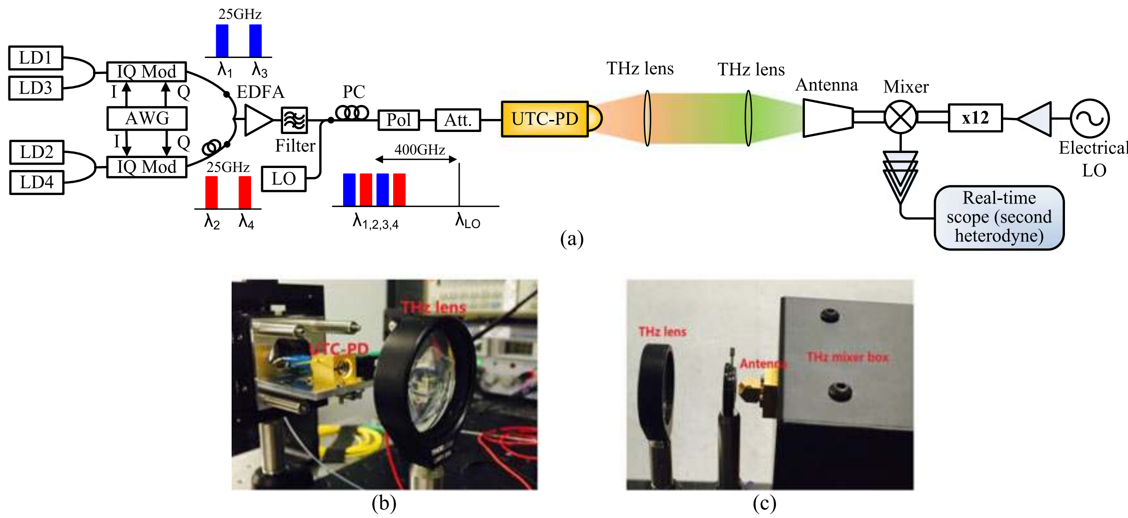

Fig. 3. (a) Experimental setup. LD: laser diode, AWG: arbitrary waveform generator, Pol: polarizer, Att.: attenuator, LO: local oscillator. (b) and (c) Photos of THz emitter and THz receiver, respectively.

real-time DSP algorithms include frequency down conversion (second heterodyne detection), bandpass filtering, I-Q separation, carrier recovery, synchronization, equalization, data recovery, and bit error rate (BER) estimation, similar as a real-time coherent receiver. Here, the BER is evaluated from the error-vector magnitude of the processed constellations.

The link budget of such a THz wireless communication system can be usually calculated by the Friis formula [32]

$$P_{Rx} = P_{Tx} + G_{Tx} + G_{Rx} - L_{\text{Free-space}}. \tag{1}$$

Here, P_{Rx} is the received power and P_{Tx} the transmitted power in dBm, G_{Tx} and G_{Rx} are the gains of transmitter and receiver in dBi respectively, and $L_{\text{Free-space}}$ represents the free space path loss in dB. In this case, the signal-to-noise ratio (SNR) for a channel with a bandwidth of B can be expressed as [33]

$$\text{SNR} = \frac{P_{Rx}}{kTB \cdot N_f} \tag{2}$$

where k is the Boltzmann constant, T is the temperature, and N_f is the receiver noise figure denoting additional noise in a nonideal receiver. From (2), it is obvious that a narrower bandwidth B (lower baud rate) naturally results in a larger SNR.

In our system, besides two antennas for the transmitter and receiver, gain of two THz lenses in the free-space propagation path is also taken into account. The estimation of link budget is illustrated in Table I. We can see the employment of 50-GHz bandwidth makes 400-GHz wireless transmission of QPSK modulation with high data rates possible in such a system. In this context, we first measure the overall system frequency response in the 370–460-GHz band, as shown in Fig. 4. It is noted that this frequency response contains the response of the UTC-PD, wireless propagation channel, as well as the THz receiver. This frequency response is measured by estimating the down-converted IF signal at 10 GHz after wireless propagation. From Fig. 4, we can see the system response fluctuation is less than 7.5 dB in the entire 370–460-GHz band.

TABLE I
400-GHz Link Budget

Parameter	Value	Unit	Remark
Bandwidth	50	GHz	
THz power	−17	dBm	400 GHz at 15-dBm optical power
Tx antenna gain	25	dBi	Estimation from the literature [14]
Free space loss	78	dB	400 GHz, 50 cm
Rx antenna gain	25	dBi	Diagonal antenna
THz lens gain	25	dBi	Two lenses in the free-space path
Received THz power	−24	dBm	
Rx loss	22	dB	THz-to-IF down-conversion loss
Received IF	−46	dBm	
IF noise floor	−63	dBm	Equivalent floor −170 dBm/Hz [12]
Rx noise figure	6	dB	Cascaded amplifiers
SNR per symbol	15	dB	BER of 1e−3, QPSK: 6.8 dB
System margin	8	dB	

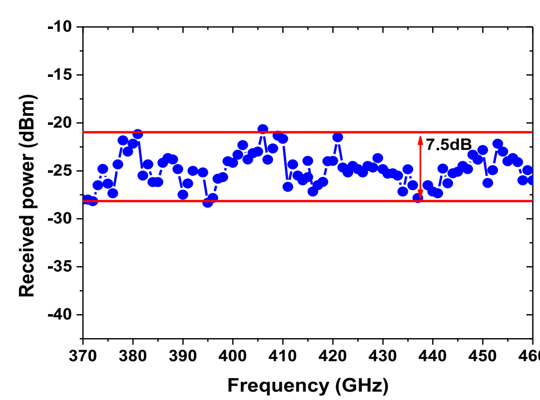

Fig. 4. System frequency response in the 370–460-GHz band.

We measure the BER performance for both single-channel and multichannel THz wireless transmission in the experiment. Different cases are experimentally demonstrated for the multichannel, including three channel and four channel, as well as line rate mixed three channel. Fig. 5 shows the BER

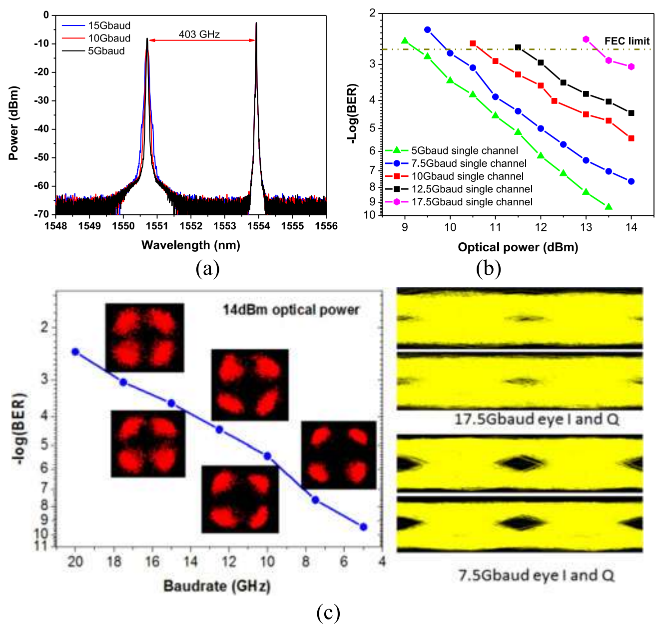

Fig. 5. (a) Optical spectrum of single THz channel at different baud rates. (b) BER performance of a single THz channel at different baud rates, (c) BER performance of a single THz channel versus baudrate. Right: I-Q eye diagrams for 17.5- and 7.5-Gbaud rates.

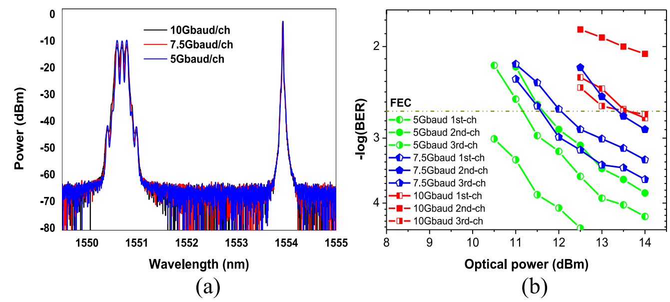

Fig. 6. (a) Optical spectrum of three-channel THz signals at different baud rates. (b) BER performance of three THz channels with 5-, 7.5-, and 10-Gbaud line rates.

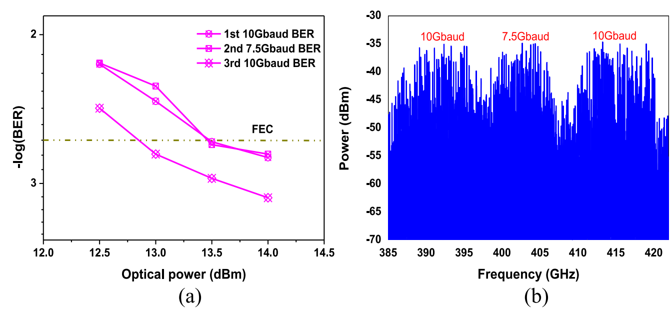

Fig. 7. (a) BER performance and (b) electrical spectrum of mixed three-channel THz signals (10, 7.5, and 10 Gbaud).

performance of single THz channel at different baud rates. The THz carrier generated from the photomixing of two CW wavelengths is 403 GHz (see optical spectrum in Fig. 5(a)). While keeping the optical power to the UTC-PD constant at 14 dBm, error-free (at BER of 1e−9) QPSK operation can be achieved at 5 Gbaud, and performance below the forward error correction (FEC, corresponding to a BER of 2e−3 with 7% overhead) at 18 Gbaud, as shown in Fig. 5(c). Higher baud rate results in more closed eye diagrams, and examples of constellation diagrams are also given in Fig. 5(c) for 7.5- to 17.5-Gbaud Nyquist QPSK signals. Fig. 5(b) displays the measured BER performance of a single THz channel versus optical power for 5 to 17.5 Gbaud. The photocurrent generated in the UTC-PD is proportional to the input optical power, and the THz emission power is proportional to the square of photocurrent, so a lower SNR is encountered at higher baud rates. BER below the FEC can be achieved for all cases here, while with a penalty at higher rates, i.e., at 10 and 10.7 dBm for 7.5 and 10 Gbaud, respectively.

Fig. 6 depicts the measured performance for three THz channels with 5-, 7.5-, and 10-Gbaud line rates, respectively. In this measurement, three 12.5 GHz-spaced carrier frequencies are 390.5, 403, and 415.5 GHz. From the optical spectra in Fig. 6(a), we can observe the optical SNR degradation when increasing the applied symbol rates, due to constant output power from the EDFA. The measured BER performance for each channel is shown in Fig. 6(b). As a result, 5-Gbaud channels have the best performance among them. In the groups with baud rates of 5 and 7.5 Gbaud, the middle channel (2nd-channel) is about 0.5 and 1 dB worse than the other two, which is induced by the crosstalk from neighboring two channels mainly caused by cross phase modulation in the EDFA. This means that within the 12.5-GHz frequency slot, higher line rates reasonably cause more crosstalk. In fact, all three channels at 5 and 7.5 Gbaud can reach the performance below the FEC. However, the middle channel of 10 Gbaud cannot due to severe crosstalk within the 12.5-GHz bandwidth. This issue can be solved by reducing the line rate for the middle channel, i.e., from 10 to 7.5 Gbaud.

Fig. 7(b) illustrates the three-channel electrical spectrum with mixed line rates. Here, the 2nd-channel carries 7.5-Gbaud QPSK data, while the 1st-channel and the 3rd-channel are at 10 Gbaud. In this context, as shown in Fig. 7(a), all three channels successfully achieve BER performance below the FEC, leading to an aggregated data rate of 55 Gb/s. We can also observe around 0.5-dB receiver penalty between the 1st- and 3rd-channels here, which is mainly caused by the imperfectly flat frequency response of the THz mixer.

Four-channel THz wireless transmission performance is shown in Fig. 8. In the experiment, four channels with 12.5-GHz wavelength spacing are modulated with 7.5-Gbaud Nyquist QPSK baseband data. The overall bitrate reaches up to 60 Gb/s. The measured optical and electrical spectra are shown in Fig. 8(a) and (b). In this case, the four carrier frequencies after photomixing are 390.5, 403, 415.5, and 428 GHz, respectively. From the BER results in Fig. 8(c), we can see performance below the FEC is achieved for all four channels, with similar performance for channels 1, 2, and 3. Compared to the three-channel BER performance at 7.5 Gbaud presented in Fig. 6(b), there is an approximately 2.5-dB receiver penalty caused by SNR degradation when the shared EDFA output power is constant. Similarly,

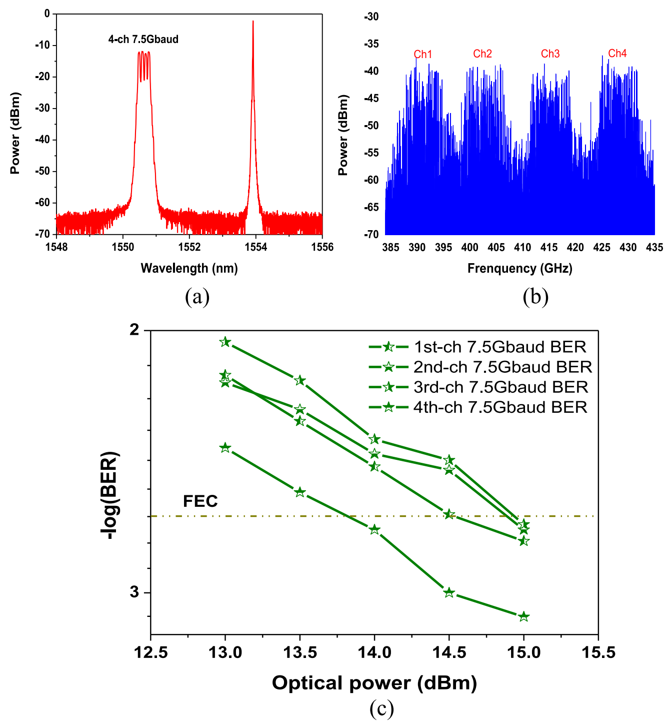

Fig. 8. (a) and (b) Optical spectrum and electrical spectrum of the four-channel THz signals with 60 Gb/s overall data rate, respectively. (c) BER performance of four THz channels after 50-cm wireless transmission.

frequency-dependent response of the THz mixer causes 0.5-dB penalty between the 4th-channel and others.

IV. Conclusion

We have successfully demonstrated a high-speed 400 GHz photonic wireless communication system with an aggregated data rate of up to 60 Gb/s. This pushes the data rate envelope enabled by optoelectronics approach at frequencies above 300 GHz. To further extend the wireless coverage of such a system, enhancement of THz link budget from the device level will be highly appreciated, specifically improvement of photodiode responsivity and receiver sensitivity, as well as development of THz amplifiers and very high-gain THz antennas. This optoelectronics scheme is fully compatible with WDM optical networks by simply inserting an additional optical heterodyne wavelength for generating high-speed THz signals by photomixing. Our system is also flexible and scalable with line rates, and the successful THz wireless transmission of Nyquist QPSK signals in a 12.5-GHz UD-WDM grid makes this scheme very promising in bridging next generation optical 100-GbE data rates into the wireless domain, for very high data rate radio wireless applications.

References

[1] (2013). [Online]. Available: http://www.ieee802.org/3/400GSG/public/13_11/chang_400_01a_1113.pdf

[2] J. Federici and L. Moeller, “Review of terahertz and subterahertz wireless communications,” *J. Appl. Phys.*, vol. 107, 2010, Art. no. 111101, pp. 1–21.

[3] J.-W. Shi, C.-B. Huang, and C.-L. Pan, “Millimeter-wave photonic wireless links for very-high data rate communication,” *NPG Asia Mater.*, vol. 3, no. 2, pp. 41–48, Apr. 2011.

[4] T. Nagatsuma *et al.*, “Terahertz wireless communications based on photonics technologies,” *Opt. Exp.*, vol. 21, no. 20, pp. 23736–23747, 2013.

[5] V. Dyadyuk *et al.*, “A multigigabit millimeter-wave communication system with improved spectral efficiency,” *IEEE Trans. Microw. Theory Techn.*, vol. 55, no. 12, pp. 2813–2821, Dec. 2007.

[6] Y. Nakasha *et al.*, “W-band transmitter and receiver for 10-Gb/s impulse radio with an optical-fiber interface,” *IEEE Trans. Microw. Theory Techn.*, vol. 57, no. 12, pp. 3171–3180, Dec. 2009.

[7] X. Pang *et al.*, “100 Gbps hybrid optical fiber-wireless link in the W-band (75-110 GHz),” *Opt. Exp.*, vol. 19, pp. 24944–24949, 2011.

[8] X. Li, J. Yu, J. Zhang, Z. Dong, F. Li, and N. Chi, “A 400G optical wireless integration delivery system,” *Opt. Exp.*, vol. 21, pp. 18812–18819, 2013.

[9] J. Takeuchi, A. Hirata, H. Takahashi, and M. Teshima, “10-Gbps bi-directional and 20-Gbps uni-directional data transmission over a 120-GHz-band wireless link using a finline ortho-mode transducer,” in *Proc. Asia–Pacific Microw. Conf.*, 2010, pp. 195–198.

[10] C. Wang, C. Lin, Q. Chen, and X. Deng, “0.14 THz high speed data communication over 1.5 kilometers,” presented at the Int. Conf. Infrared Millimeter, THz Waves, Wollongong, NSW, Australia, 2012, Paper Tue-A-2-4.

[11] A. Kanno *et al.*, “Optical and millimeter-wave radio seamless MIMO transmission based on a radio over fiber technology,” *Opt. Exp.* vol. 20, no. 28, pp. 29395–29403, 2012.

[12] A. J. Seeds, H. Shams, M. Fice, and C. Renaud, “Terahertz photonics for wireless communications,” *J. Lightw. Technol.*, vol. 33, no. 3, pp. 579–587, Feb. 2015.

[13] S. Koenig *et al.*, “Wireless sub-THz communication system with high data rate,” *Nature Photon. Lett.*, vol. 7, pp. 977–981, 2013.

[14] H.-J. Song, K. Ajito, Y. Muramoto, A. Wakatsuki, T. Nagatsuma, and N. Kukutsu, “24 Gbps data transmission in 300 GHz band for future terahertz communications,” *Electron. Lett.*, vol. 48, vol. 15, pp. 953–954, 2012.

[15] G. Ducournau *et al.*, “Ultrawide-bandwidth single-channel 0.4-THz wireless link combining broadband quasi-optic photomixer and coherent detection,” *IEEE Trans. THz Sci. Technol.* vol. 4, no. 3, pp. 328–337, May 2014.

[16] K. Ishigaki, M. Shiraishi, S. Suzuki, M. Asada, N. Nishiyama, and S. Arai, “Direct intensity modulation and wireless data transmission characteristics of terahertz-oscillating resonant tunnelling diodes,” *Electron. Lett.*, vol. 48, no. 10, pp. 582–583, 2012.

[17] G. Ducournau *et al.*, “High-definition television transmission at 600 GHz combining THz photonics hotspot and high-sensitivity heterodyne receiver,” *Electron. Lett.*, vol. 50, no. 5, pp. 413–415, 2014.

[18] L. Moeller, J. Federici, and K. Su, “2.5 Gbps duobinary signalling with narrow bandwidth 0.625 terahertz source,” *Electron. Lett.*, vol. 47, no. 15, pp. 856–858, 2011.

[19] X. Yu *et al.*, “60 Gbit/s 400 GHz wireless transmission,” presented at the Photon. Switching Conf., Florence, Italy, 2015.

[20] X. Pang *et al.*, “25 Gbps QPSK hybrid fiber-wireless transmission in the W-Band (75-110GHz) with remote antenna unit for in-building wireless networks,” *IEEE Photon. J.*, vol. 4, no. 3, pp. 691–698, Jun. 2012.

[21] J. Antes *et al.*, “Transmission of an 8-PSK modulated 30 Gbit/s signal using an MMIC-based 240 GHz wireless link,” presented at the IEEE MTT-S Int. Microw. Symp., Seattle, WA, USA, 2013.

[22] J. Antes *et al.*, “220 GHz wireless data transmission experiments up to 30Gbit/s,” presented at the IEEE MTT-S Int. Microw. Symp., Montreal, QC, Canada, 2012.

[23] G. Ducournau *et al.*, “THz communications using photonics and electronic devices: The race to data-rate,” *J. Infrared Millimeter THz Waves*, vol. 36, pp. 198–218, 2015.

[24] F. Boes *et al.*, “Ultra-broadband MMIC-based wireless link at 240 GHz enabled by 64 GS/s DAC,” presented at the 39th Int. Conf. Infrared, Millimeter, THz Waves, Tucson, AZ, USA, 2014.

[25] I. Kallfass *et al.*, “Towards MMIC-based 300 GHz indoor wireless communication systems,” *IEICE Trans. Electron.*, vol. E98-C, no. 12, pp. 1081–1090, 2015.

[26] T. Nagatsuma and G. Carpintero, “Recent progress and future prospect of photonics-enabled terahertz communications research,” *IEICE Trans. Electron.*, vol. E98-C, no. 12, pp. 1060–1070, 2015.
[27] H. Shams, M. J. Fice, K. Balakier, C. C. Renaud, F. van Dijk, and A. J. Seeds, “Photonic generation for multichannel THz wireless communication,” *Opt. Exp.*, vol. 22, no. 19, pp. 23465–23472, 2014.
[28] G. Ducournau *et al.*, “32 Gbps QPSK transmission at 385 GHz using coherent fibre-optic technologies and THz double heterodyne detection,” *Electron. Lett.*, vol. 51, no. 12, pp. 915–917, 2015.
[29] [Online]. Available: http://www.huawei.com/ilink/en/solutions/broader-smarter/morematerial-b/HW_104782
[30] H. Ito, T. Yoshimatsu, H. Yamamoto, and T. Ishibashi, “Widely frequency tunable terahertz-wave emitter integrating uni-traveling-carrier photodiode and extended bowtie antenna,” *Appl. Phys. Exp.*, vol. 6, no. 6, pp. 064101-1–064101-3, 2013.
[31] (2014). [Online]. Available: http://literature.cdn.keysight.com/litweb/pdf/5990-7451EN.pdf
[32] H. T. Friis, “A note on a simple transmission formula,” *Proc. IRE*, vol. 34, no. 5, pp. 254–256, May 1946.
[33] T. Schneider, A. Wiatrek, S. Preußler, M. Grigat, and R.-P. Braun, “Link budget analysis for terahertz fixed wireless links,” *IEEE Trans. THz Sci. Technol.*, vol. 2, no. 2, pp. 250–256, Mar. 2012.

Xianbin Yu (M’09–SM’15) received the M.Sc. degree from Tianjin University, Tianjin, China, in 2002, and the Ph.D. degree from Zhejiang University, Hangzhou, China, in 2005.

From October 2005 to October 2007, he was a Postdoctoral Researcher with Tsinghua University, Beijing, China. Since November 2007, he has been with the Technical University of Denmark, Kgs. Lyngby, Denmark, as a Postdoctoral Fellow, Assistant Professor, and Senior Researcher. He is currently a Research Professor with Zhejiang University. He has coauthored 2 book chapters and more than 120 peer-reviewed international journal and conference papers in the area of optical communications. His research interests include THz/microwave photonics, optical fiber communications, ultrafast photonic wireless signal processing, and ultrahigh frequency wireless fiber access technologies.

Dr. Yu held a Marie Curie Fellowship within the 7th European Community Framework Program (2009–2011).

Rameez Asif, photograph and biography not available at the time of publication.

Molly Piels, photograph and biography not available at the time of publication.

Darko Zibar, photograph and biography not available at the time of publication.

Michael Galili, photograph and biography not available at the time of publication.

Toshio Morioka, photograph and biography not available at the time of publication.

Peter U. Jepsen, photograph and biography not available at the time of publication.

Leif K. Oxenløwe, photograph and biography not available at the time of publication.